Single-molecule analysis of chemoattractant-stimulated membrane recruitment of a PH-domain-containing protein

Satomi Matsuoka[1], Miho Iijima[2], Tomonobu M. Watanabe[1], Hidekazu Kuwayama[1], Toshio Yanagida[1], Peter N. Devreotes[2] and Masahiro Ueda[1,*]

[1]Laboratories for Nanobiology, Graduate School of Frontier Biosciences, Osaka University, 1-3 Yamadaoka, Suita, Osaka, 565-0871, Japan
[2]Department of Cell Biology, Johns Hopkins University School of Medicine, 725 N. Wolfe St., 114 WBSB, Baltimore, Maryland, 21205, USA
*Author for correspondence (e-mail: ueda@phys1.med.osaka-u.ac.jp)

Accepted 22 November 2005
Journal of Cell Science 119, 1071-1079 Published by The Company of Biologists 2006
doi:10.1242/jcs.02824

Summary

Molecular mechanisms of chemotactic response are highly conserved among many eukaryotic cells including human leukocytes and *Dictyostelium discoideum* cells. The cells can sense the differences in chemoattractant concentration across the cell body and respond by extending pseudopods from the cell side facing to a higher concentration. Pseudopod formation is regulated by binding of pleckstrin homology (PH)-domain-containing proteins to phosphatidylinositol 3,4,5-trisphosphates [PtdIns(3,4,5)P_3] localized at the leading edge of chemotaxing cells. However, molecular mechanisms underlying dynamic features of a pseudopod have not been fully explained by the known properties of PH-domain-containing proteins. To investigate the mechanisms, we visualized single molecules of green fluorescent protein tagged to Crac (Crac-GFP), a PH-domain-containing protein in *D. discoideum* cells. Whereas populations of Crac molecules exhibited a stable steady-state localization at pseudopods, individual molecules bound transiently to PtdIns(3,4,5)P_3 for ~120 milliseconds, indicating dynamic properties of the PH-domain-containing protein. Receptor stimulation did not alter the binding stability but regulated the number of bound PH-domain molecules by metabolism of PtdIns(3,4,5)P_3. These results demonstrate that the steady-state localization of PH-domain-containing proteins at the leading edge of chemotaxing cells is dynamically maintained by rapid recycling of individual PH-domain-containing proteins. The short interaction between PH domains and PtdIns(3,4,5)P_3 contributes to accurate and sensitive chemotactic movements through the dynamic redistributions. These dynamic properties might be a common feature of signaling components involved in chemotaxis.

Supplementary material available online at
http://jcs.biologists.org/cgi/content/full/119/6/1071/DC1

Key words: Single-molecule imaging, Plekstrin homology domain, Phosphatidylinositol 3,4,5-trisphosphate, Chemotaxis, Cell polarity

Introduction

Directional motile responses of living organisms to chemical gradients are referred to as chemotaxis, a process by which organisms sense gradients and move with directional preference towards or away from a source of chemical cues. Chemotaxis of eukaryotic cells occurs during a variety of physiological and pathological processes including immunity, neuronal patterning, morphogenesis and nutrient finding. Recent investigations of the molecular and cellular biology of the chemotactic response have demonstrated that the molecular mechanisms are largely shared among many eukaryotic cells, including human leukocytes and the social amoebae *Dictyostelium discoideum* (Devreotes and Zigmond, 1988; Kimmel and Parent, 2003; Ridley et al., 2003; Postma et al., 2004a; Parent, 2004).

Eukaryotic cells sense the differences in chemoattractant concentration across the cell body and respond by extending pseudopodia towards the high-concentration end of the gradient (Devreotes and Zigmond, 1988; Parent and Devreotes, 1999). In *D. discoideum* amoebae, extracellular 3′-5′-cyclic adenosine monophosphate (cAMP) functions as a chemoattractant. Differences in the concentration of cAMP across the cell of only ~2% is sufficient to trigger chemotactic movements (Mato et al., 1975; Fisher et al., 1989). Thus, chemotactic signaling systems can convert small differences in extracellular signals into localized responses that form pseudopodia predominantly at the cell side facing the higher concentration of chemoattractant.

The chemotactic signaling system of *D. discoideum* cells consists of cAMP receptors (cARs), their coupled trimeric G-proteins and downstream signaling molecules including phosphatidylinositol 3-kinase (PI 3-K), PTEN, plekstrin homology (PH)-domain-containing proteins such as Crac and protein kinase B (Kimmel and Parent, 2003). Imaging analyses of these signaling molecules using a green fluorescent protein (GFP) has revealed differences in the intracellular localization of these signaling molecules in response to chemotactic stimulation. Receptors and G-protein α- and βγ-subunits are distributed almost uniformly along the cell surface during chemotaxis (Xiao et al., 1997; Jin et al., 2000; Janetopoulos et

al., 2001). By contrast, PI 3-K and PTEN, which control the production and degradation of phosphatidylinositol 3,4,5-trisphosphates [PtdIns(3,4,5)P_3], are highly localized at the leading edge and the rear end of chemotaxing cells, respectively (Iijima and Devreotes, 2002; Funamoto et al., 2002). The complementary distribution of PI 3-K and PTEN leads to the accumulation of PtdIns(3,4,5)P_3 at the leading edge of chemotaxing cells (Comer and Parent, 2002; Iijima et al., 2002; Huang et al., 2003). The PtdIns(3,4,5)P_3 on the membrane of chemotaxing cells provides binding sites for PH-domain-containing proteins (Dormann et al., 2004). In fact, PH-domain-containing proteins such as Crac and protein kinase B are highly localized at the leading edge of *D. discoideum* cells during chemotaxis (Parent et al., 1998; Meili et al., 1999). Similar localizations of PH-domain-containing proteins have been observed in mammalian leukocytes and fibroblasts (Servant et al., 2000; Haugh et al., 2000). Thus, chemical gradients of extracellular signals lead to localization of PtdIns(3,4,5)P_3-bound PH-domain-containing proteins to the leading edge of the cell.

Since the regions where PH-domain-containing proteins accumulate correspond to the sites of pseudopod formation, PH-domain-containing proteins have been suggested to be key molecules that regulate the localized activation of actin polymerization in *D. discoideum* and leukocytes (Iijima et al., 2002; Huang et al., 2003; Bourne and Weiner, 2002; Postma et al., 2004b; Comer et al., 2005). To understand how PH-domain-containing proteins transmit the localized signals of PtdIns(3,4,5)P_3 to downstream signaling pathways, it is important to determine the binding properties of PH-domain-containing proteins to PtdIns(3,4,5)P_3 in living cells during chemotaxis. For example, stable Crac molecules are observed continuously at the pseudopod of chemotaxing cells, but the molecules rapidly localize in response to directional changes of external gradients (Parent and Devreotes, 1999; Parent et al., 1998; Meili et al., 1999). The entire molecular process from stimulation with cAMP to pseudopod formation can occur within a few seconds (Swanson and Taylor, 1982). The underlying molecular mechanism for such stable localization and rapid reorientation of Crac has not been established.

Crac was originally identified as a cytosolic regulator of adenylyl cyclase, a signaling molecule important for intercellular relay of cAMP (Insall et al., 1994; Lilly and Devreotes, 1994; Lilly and Devreotes, 1995; Wang et al., 1999). Interestingly, Crac is highly localized at the leading edge pseudopod of chemotaxing cells, whereas its effector adenylyl cyclase A (ACA) is localized at the tail of the cell (Parent et al., 1998; Kriebel et al., 2003). Thus, it is important to determine how Crac contributes to the activation of ACA and whether Crac interacts with ACA at the rear tail of chemotaxing cells.

We have developed single-molecule fluorescence imaging techniques in living cells (Funatsu et al., 1995; Tokunaga et al., 1997; Sako et al., 2000a; Ueda et al., 2001). Fluorescence from single GFP molecules is strong enough to be observed at the single-molecule level in living cells (Sako et al., 2000b; Iino et al., 2001; Watanabe and Mitchison, 2001; Hibino et al., 2003). The techniques have been successfully used to visualize unitary reactions in signal transduction such as ligand binding, receptor dimerization, phosphorylation, diffusion and membrane recruitment of signaling molecules in the context of an intracellular environment; thereby molecular mechanisms underlying signal transduction have emerged (Ishijima and Yanagida, 2001; Sako and Yanagida, 2003). Single-molecule imaging techniques also can detect rare and minor events concerning the signaling molecules that are obscured in the ensemble measurements containing a large number of molecules.

In this study, we visualized in living *D. discoideum* cells single molecules of Crac fused to GFP (Crac-GFP). The results demonstrate that individual Crac molecules do not bind stably to PtdIns(3,4,5)P_3 but exchange at an order of ~100 milliseconds, indicating that a steady-state localization of PH-domain-containing proteins at the leading edge pseudopod is maintained dynamically by the rapid exchanges of the individual molecules. These properties of PH-domain-binding provide a molecular basis for the rapid reorientation of the region of highest accumulation in response to directional changes of chemical gradients. Additionally, we found further minor sites for Crac to bind on membranes that were proven to be ACA-dependent localized preferentially at the rear end of chemotaxing cell, suggesting that sub-populations of Crac molecules serve as a regulator for ACA in chemotaxing cells.

Results

Translocations of Crac-GFP in living cells observed with standard epifluorescence microscopy

The behavior of Crac-GFP in response to chemotactic stimulation in living cells observed with standard epifluorescence microscopy (EPI-FM) has been described previously (Parent et al., 1998; Postma et al., 2004b; Janetopoulos et al., 2004). Briefly, before the stimulation with cAMP, Crac-GFP is localized mainly in the cytosol (Fig. 1). When cells are stimulated uniformly with cAMP, Crac-GFP is recruited transiently to almost the entire surface of membrane, which is visualized by the change in fluorescence intensity of Crac-GFP on membranes. Typically, the recruitment of Crac-GFP to membranes peaks at 5-10 seconds after stimulation with cAMP (Fig. 1B) and is followed by a second phase of binding to patches over the next several minutes (data not shown). In response to a concentration gradient of cAMP, cells adopt a polarized shape with pseudopodia directed towards the high-concentration end of the gradient (Fig. 1C). Crac-GFP is localized persistently at the pseudopod of chemotaxing cells. In response to a change in orientation of the gradient, the localization of Crac-GFP is rapidly reoriented towards the new direction accompanied by pseudopod formation. Thus, Crac-GFP serves as a reporter of the localized signal for pseudopod formation elicited by stimulation with cAMP.

Single-molecule visualization of Crac-GFP by using a total internal reflection fluorescence microscopy

We visualized single molecules of Crac-GFP in living cells using total internal reflection fluorescence microscopy (TIR-FM) (Fig. 2A,B). Cells expressing Crac-GFP were placed on coverslips and overlaid with a thin agarose sheet (Fukui et al., 1987). With this agar-overlay, the basal surface of the cells is in close proximity to the surface of the coverslip. This is crucial for single-molecule imaging because the excitation light for GFP extends only a short distance beyond the surface of the coverslip (Ueda et al., 2001; Axelrod, 2001; Wazawa and Ueda, 2005).

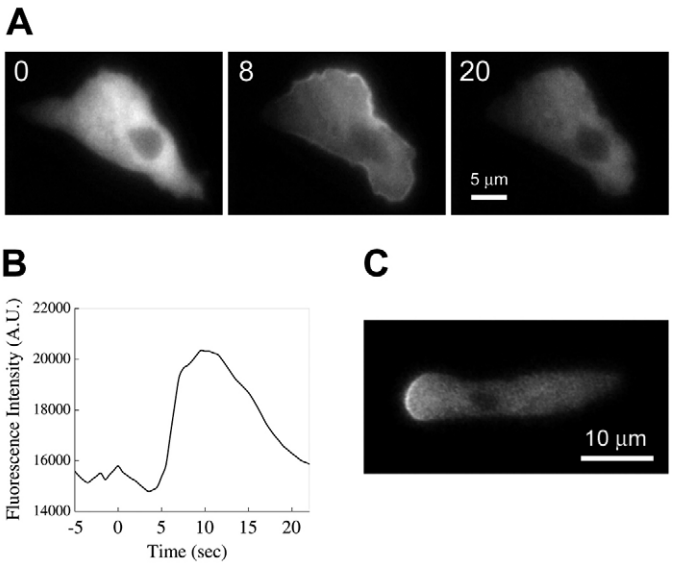

Fig. 1. Translocation of Crac-GFP to membranes in *D. discoideum* cells after stimulation with cAMP. Images in A and C show one cell. (A) *D. discoideum* cells were stimulated at t=0 seconds with a uniform concentration of cAMP. Standard epifluorescence images were taken at 30 images per second. Before stimulation with cAMP Crac-GFP was distributed in the cytosol. After stimulation it translocated uniformly and almost entirely to the cell surface. (B) Time course of the Crac-GFP recruitment shown in A. Fluorescence intensities of Crac-GFP on membranes were measured and plotted over time. Fluorescence intensities were calibrated by using the photobleaching rates of GFP. (C) Localization of Crac-GFP at the leading-edge pseudopod of cells in gradients of cAMP.

Fig. 2C shows a typical example of fluorescent spots arising from Crac-GFP bound to basal membrane of living cells. To confirm that the fluorescent spots represent single Crac-GFP molecules, we examined the fluorescence intensity and photobleaching characteristics of the spots (Fig. 2D-H). The fluorescence intensities of Crac-GFP in living cells were comparable to those of GFP molecules adsorbed randomly onto a glass surface (Fig. 2D). The fluorescence of Crac-GFP adsorbed onto a glass surface disappeared in a single step, as expected from photobleaching reactions of single GFP molecules (Fig. 2E) (Funatsu et al., 1995; Sako et al., 2000b; Ueda et al., 2001). We have sometimes observed on/off blinking of Crac-GFP adsorbed onto a glass surface, which is also an indication of successful imaging of single GFP molecules (Dickson et al., 1997). The lifetime of Crac-GFP absorbed onto a glass surface was ~3.8 seconds, indicating that the photobleaching rate of GFP in our experimental system was ~0.33 seconds.

Cytosolic Crac-GFP is not imaged clearly as a fluorescent spot at video frame rates, because of rapid Brownian motion of the Crac-GFP in the cytosol. However, when Crac-GFP binds to a membrane, diffusion movements of Crac-GFP become slower because of this association, and visualization of the GFP fluorescence as a single spot becomes possible. Following the release of the Crac-GFP molecule from the membrane, the fluorescent spot suddenly disappears. Thus, only membrane-bound Crac-GFP molecules are visualized in living cells. In cells expressing GFP alone, fluorescent spots were very infrequently observed on the membrane, indicating specific binding of Crac-GFP to membranes (Fig. 2C). The fluorescence emitted from cytosolic Crac-GFP and GFP alone appeared as obscure fluorescence in the background. However, it was easily distinguished from fluorescent spots of membrane-bound Crac-GFP, because the fluorescence of a single molecule can be visualized as a spot of ~0.5 μm in size (Fig. 2F) (Funatsu et al., 1995; Sako et al., 2000b; Ueda et al., 2001). Smaller spots, which appeared and disappeared very suddenly within ~33 milliseconds, are shot noises that arose due to the stochastic nature of photoelectrons produced during the image-intensifying process.

To make ensure that the fluorescent spots observed in living cells represent single Crac-GFP molecules, photobleaching characteristics of the spots were examined in fixed cells, in which membrane-bound molecules can no longer move or dissociate from the membrane (Fig. 2G). Under those conditions, disappearance of the fluorescent spot should result from photobleaching of the fluorophore. Indeed, the lifetime of immobilized Crac-GFP molecules on the cell membrane was ~4 seconds, which is consistent with the lifetime of a Crac-GFP molecule absorbed onto the coversip. The fluorescent spots showed the single-step-bleaching characteristics, and the size of these spots were ~ 0.5 μm (Fig. 2G,H). These are strong evidences that fluorescent spots observed in cells expressing Crac-GFP represent single Crac-GFP molecules and provide good reason to attribute the ~0.5 μm fluorescent spots to single Crac-GFP molecules in living cells.

When the cells were stimulated with low concentrations of cAMP, the number of Crac-GFP spots on the membranes increased transiently (Fig. 3A; supplementary material, Movies 1 and 2). By counting the number of Crac-GFP spots, we obtained the time course of Crac recruitment, induced by stimulation with cAMP (Fig. 3B). It begins ~4 seconds after stimulation, reaches a plateau and is then sustained for ~10 seconds before returning to the basal level within 20 seconds after stimulation. This time course is comparable to that observed for Crac-GFP using EPI-FM (Fig. 1B) (Parent et al., 1998; Postma et al., 2004b). Although observation with TIR-FM is limited to the basal membrane of cells, essentially the same reactions observed with EPI-FM can be detected by this method.

Rapid exchange of Crac-GFP molecules on membranes

With standard EPI-FM, the fluorescence signals arising from Crac-GFP appeared on membranes continuously for ~10 seconds in response to a sudden increase in the extracellular concentration of cAMP (Fig. 1A). However, the single-molecule observation reveals that individual Crac-GFP molecules only transiently associate with the membrane (Fig. 3A; supplementary material Movies 1 and 2). We measured the time from the initial observation to the disappearance of individual Crac-GFP molecules (lifetime), and plotted this data as a cumulative curve over time (Fig. 3C). The curve represents the probability of binding as a function of time, the dissociation curve for Crac-GFP. By fitting the curve to a single exponential function, the time-constant of dissociation τ can be obtained (Ueda et al., 2001; Sakmann and Neher, 1995). In the case of Crac-GFP the τ value after stimulation with cAMP was τ=120 milliseconds (Fig. 3C, ●). Since the lifetime of GFP photobleaching was ~4 seconds (Fig. 3C, ▲), we concluded

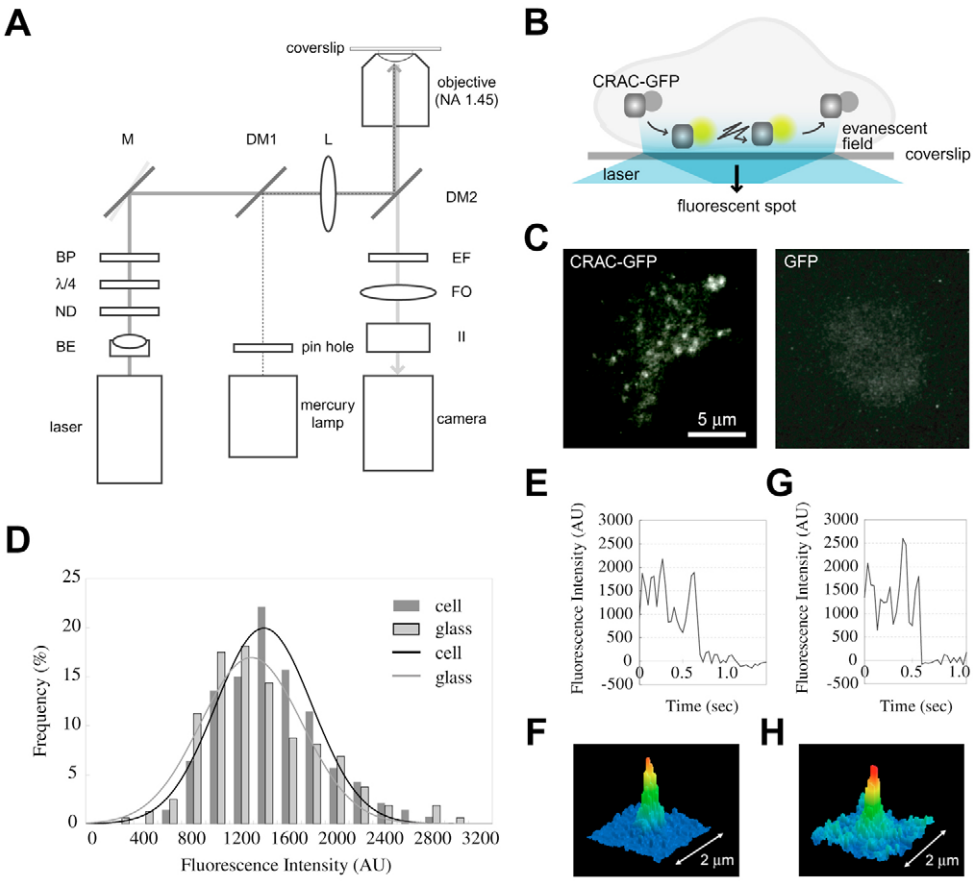

Fig. 2. Single-molecule imaging of Crac-GFP in living *D. discoideum* cells. (A) Configuration of a total internal reflection fluorescence microscope (TIR-FM) for single-molecule imaging attached to an inverted microscope (IX-70, Olympus Inc, Japan). (B) Schematic illustration of single-molecule imaging of Crac-GFP bound to the basal membranes of a *D. discoideum* cell that is illuminated by evanescent fields generated by TIR of excitation light on the surface of a coverslip. (C) Typical images of Crac-GFP visualized by TIR-FM (left panel). Fluorescent spots were hardly detected in a cell expressed GFP alone (right panel). (D) Histogram of fluorescence intensities of the spots of Crac-GFP observed in living cells (dark gray bars) and on the surface of coverslips (light gray bars). Each distribution was fitted to an Gaussian function. (E) An example of a single-step photobleaching of Crac-GFP on coverslips. (F) An intensity profile of a fluorescent spot representing a single Crac-GFP molecule attached to a coverslip. (G) An example of a single-step photobleaching of Crac-GFP in fixed cells. (H) An intensity profile of a fluorescent spot representing a single Crac-GFP molecule in a fixed cell. The background fluorescence was heterogeneous when compared to (F), which came from unbound Crac-GFP molecules present in the cytosol.

that Crac-GFP molecules dissociate from membranes without photobleaching. Thus, populations of Crac-GFP molecules on membranes appear continuously for ~10 seconds, but individual Crac-GFP molecules are exchanged rapidly on membranes. Transient increments of Crac-GFP on membranes elicited by stimulation with cAMP are the sum of single binding events by individual Crac-GFP molecules.

Two binding sites for Crac-GFP and the effects of cAMP stimulation

To investigate whether stimulation with cAMP regulates the lifetime of Crac-GFP on membranes, we examined the binding properties of Crac-GFP on unstimulated, stimulated, or adapted cells, following stimulation with cAMP. In unstimulated and adapted cells, the steady-state number of bound Crac-GFP was very low but was detectable above the number of background spots observed with GFP. As shown in Fig. 4B, the dissociation curves of Crac-GFP in unstimulated cells were fitted well to a sum of two exponential functions, indicating the presence of at least two different sites for Crac-GFP binding; their dissociation half-times were 150 milliseconds (87%) and 910 milliseconds (13%). Similarly, the adapted cells had two different kinetic sites after stimulation with cAMP: 150 milliseconds (86%) and 1090 milliseconds (14%). In both cases, the rate of the rapid dissociation site was similar to the single site observed in stimulated cells (Fig. 3B, Fig. 4B). This suggests that cAMP stimulation selectively increased the number of 'rapid' sites on membranes.

Since it has been demonstrated that Crac-GFP molecules bind to PtdIns(3,4,5)P_3 on membranes through a PH-domain (Huang et al., 2003), we measured the dissociation rates of PH_{Crac}-GFP, in which the PH-domain of Crac is fused to GFP (Fig. 4B, ●). After stimulation with cAMP the cells showed a transient localization of PH_{Crac}-GFP to the membrane with the same time course as Crac-GFP. The dissociation curve of PH_{Crac}-GFP could be fitted to a single exponential function with a time constant of 120 milliseconds irrespective of whether or not the cells were stimulated with cAMP. This result indicates that the rapid site is PtdIns(3,4,5)P_3. The slow-dissociation site was not detected by PH_{Crac}-GFP, suggesting that the slow-dissociation site probably involves interaction with additional domains of Crac.

Crac in polarized cells that undergo chemotaxis

We next examined the binding properties of Crac-GFP to membranes in cells that undergo chemotaxis. Chemotaxing cells typically have a polarized shape with a pseudopod at the leading edge and a tail at the rear (Fig. 5A; supplementary material Movies 3 and 4). Consistent with previous reports (Parent et al., 1998), Crac-GFP molecules were enriched at the leading edge of the cells. At the leading edge, almost all of the Crac-GFP dissociated from the membrane with a time

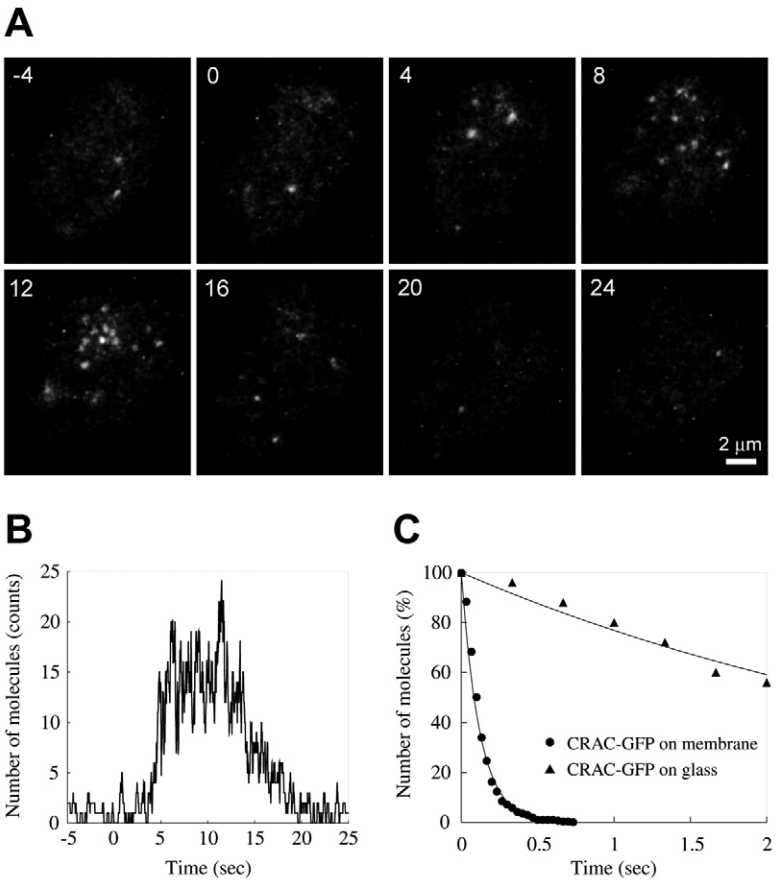

Fig. 3. Single-molecule imaging of the transient translocation of Crac-GFP to membranes upon stimulation with cAMP. (A) Sequential images of a cell expressing Crac-GFP observed under TIR-FM (see supplementary material Movie 1). The cell was stimulated at 0 seconds with cAMP. (B) Temporal changes in the number of Crac-GFP spots on membrane. After stimulation with cAMP, the number of the Crac-GFP spots increased transiently ~10 second. (C) Dissociation of Crac-GFP from membranes of cells stimulated with cAMP. Lifetimes of Crac-GFP between initial observation and disappearance on membrane were measured and plotted as a cumulative curve, giving rise to the dissociation curve. The data can be fitted to single exponential curve with a constant (τ) of 120 milliseconds, indicating rapid exchanges of individual Crac molecules during Crac recruitments. Dissociation curve of Crac-GFP in living cells with τ=120 milliseconds (●) and photobleaching curve of Crac-GFP absorbed on the surface of coverslip with τ=3800 milliseconds (▲).

constant of 110 milliseconds, indicating that the binding partner at the pseudopod is PtdIns(3,4,5)P_3. During the membrane association, individual Crac-GFP molecules diffused on the membrane independently of each other, showing no clustering. Thus, persistent localization of PH-domain-containing proteins at the pseudopod is maintained dynamically with rapid exchanges of the individual PH-domain-containing proteins. Furthermore, we found that Crac-GFP molecules also bind to membranes at the rear regions (Fig. 5A: arrowheads; supplementary material Movie 3), although the number of spots was ~30 times lower than that observed in the anterior region. Dissociation rates of Crac-GFP at the posterior end were 110 milliseconds (76%) and 890 milliseconds (24%) (Fig. 5B). Thus, fast-dissociation and slow-dissociation sites were preferentially localized at the leading edge and at the rear end of the polarized cells, respectively.

The fast-dissociation and slow-dissociation sites could be distinguished also by the lateral diffusion of Crac-GFP on membranes, their diffusion constants were 0.14±0.06 and 0.04±0.02 $\mu m^2/s$, respectively. These values are consistent with the idea that the binding partner comprising the slow-dissociation site is an integral protein (Jacobson et al., 1987; Saxton and Jacobson, 1997).

Crac binding to membranes in cells lacking ACA

Parent and colleagues report that ACA is localized preferentially at the posterior region of the polarized cell in a gradient of a chemoattractant (Kriebel et al., 2003). Since Crac is an essential regulator of ACA, there is a possibility that the slower binding of Crac to posterior membranes reflects on the interaction of Crac with ACA itself or with a complex that depends on the presence of ACA. We examined the membrane binding of Crac-GFP in cells lacking ACA (*aca*-null cells). The dissociation curve of Crac-GFP in *aca*-null cells was fitted to a single exponential curve with a time constant of 120 milliseconds, indicating that only one of the binding partners, PtdIns(3,4,5)P_3, is present (Fig. 6). The slow-dissociation site was not observed in the *aca*-null cells. These results strongly suggest that the binding partner for Crac with slower dissociation rates is either ACA itself or a complex that is ACA-dependent. Consistent with these observations, polarized *aca*-null cells that undergo chemotaxis do not have the slow-dissociation site for Crac-GFP at the posterior regions (data not shown).

Discussion

Single-molecule imaging of Crac-GFP in living *D. discoideum* cells revealed two different binding sites: PtdIns(3,4,5)P_3 and ACA-dependent sites, which have fast (~100 milliseconds) and slow (~1 second) dissociation rates for Crac, respectively. The binding to PtdIns(3,4,5)P_3 is achieved only through the PH-domain of Crac, whereas the binding to the ACA-dependent site required additional domains of Crac. The fast-dissociation site (PtdIns(3,4,5)P_3) was preferentially localized at the leading edge of the cell undergoing chemotaxis, and was maintained by a rapid cycling of individual Crac molecules. The ACA-dependent site was found preferentially at the rear end of the cell undergoing chemotaxis.

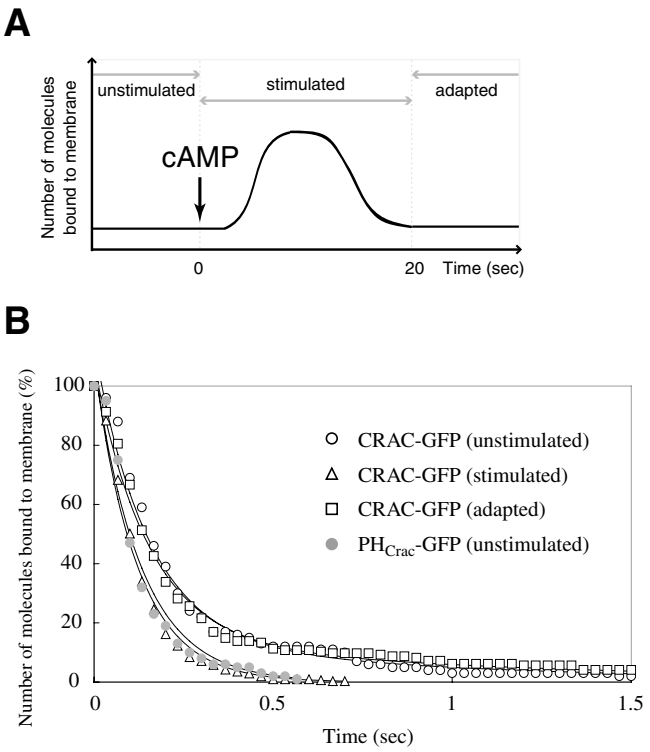

Fig. 4. Two binding sites for Crac-GFP in living cells. (A) Three states of cells; cells before stimulation, 0 to 20 seconds after stimulation, and more than 20 seconds after stimulation were referred as unstimulated, stimulated and adapted, respectively. (B) Dissociation curves of Crac-GFP and PH_{Crac}-GFP bound to the membranes. Lifetime of Crac-GFP was measured in the cells before stimulation (○), at 0-20 seconds (△) and more than 20 seconds (□) after stimulation with cAMP. The curves were fitted to a sum of exponentials with the time constant τ and the relative ratios (see Results). The lines represent the fitting curves. Dissociation curve of PH_{Crac}-GFP (●) bound to the membrane of resting cells demonstrates that the fast-dissociation site is PtdIns(3,4,5)P_3.

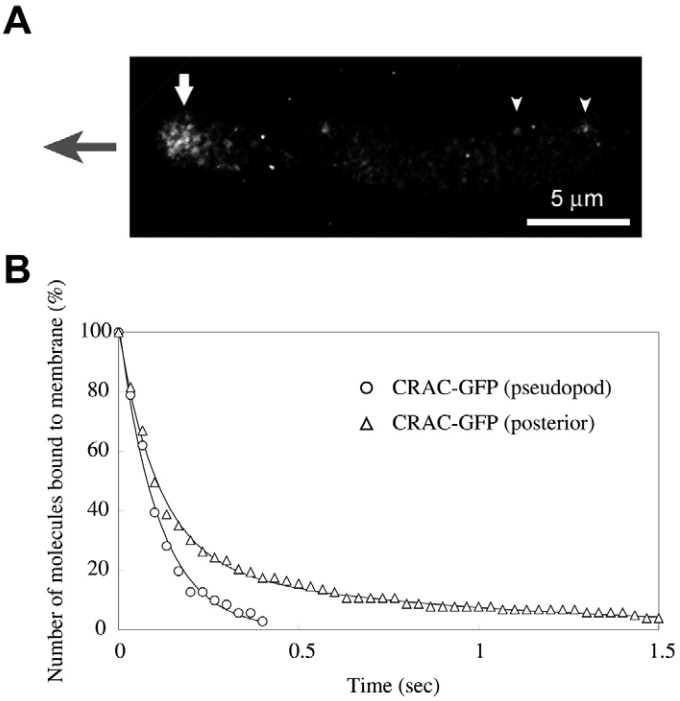

Fig. 5. Single-molecules of Crac-GFP in polarized cells undergoing chemotaxis. (A) Chemotactic cells expressing Crac-GFP were observed under TIR-FM (see supplementary material Movie 2). Crac molecules on membranes were predominantly observed at the leading edge pseudopod (white arrow), as expected from previous works (Parent et al., 1998). Arrowheads represent Crac-GFP found at the rear end of cells. The gray arrow indicates the direction of cell movement. (B) Dissociation curves of Crac-GFP bound to the pseudopod (○) or posterior region (△) were fitted to a single exponential curve with a constant of 110 milliseconds and a sum of two exponentials with constants of 110 milliseconds (72%) and 890 milliseconds (28%), respectively.

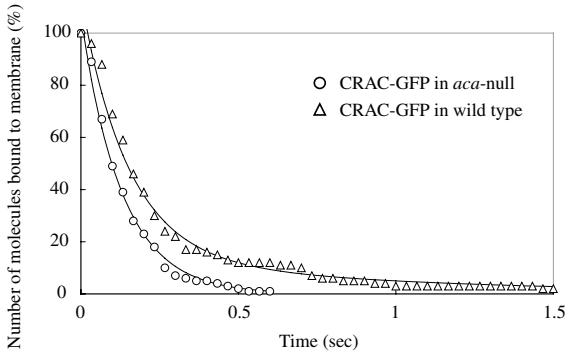

Fig. 6. Membrane binding of Crac-GFP in cells lacking ACA. Dissociation curves of Crac-GFP in wild-type (△) and *aca*-null cells (○). Cells that lack ACA have only a fast-dissociation site but lack the slow-dissociation site for Crac-GFP, suggesting that the slow-dissociation site is either ACA itself or an ACA-dependent molecule on membranes.

Single Crac-GFP molecules bound to PtdIns(3,4,5)P_3 for only a few hundred milliseconds, a property of PH-domain-containing proteins that is consistent with the dynamic behavior of populations. Previous studies have reported that the distribution of Crac-GFP rapidly readjusts following the repositioning of a micropipette containing cAMP along the cell periphery (Parent and Devreotes, 1999; Parent et al., 1998). This redistribution of Crac-GFP takes place within seconds. Rapid redistribution requires a rapid disappearance from the old localization site. Persistent binding of Crac to PtdIns(3,4,5)P_3 would prevent rapid re-orientation upon the directional change of gradient. Redistribution by lateral diffusion of the PtdIns(3,4,5)P_3-PH-domain complex on the membrane would be expected to be relatively slow. Lateral diffusion of lipid-protein complex on membranes is slower than free diffusion of soluble proteins in the cytosol (Ruchira et al., 2004). In addition, localization of the PtdIns(3,4,5)P_3-PH-domain complex would be less distinct owing to a longer duration of lateral diffusion on membrane, resulting in broadening signals transmitted by PH-domain-containing proteins. Indeed, our measurements showed that, with a diffusion coefficient of ~0.1 μm^2/second, it would take 17 minutes for the complexes to redistribute across the cell. Thus, a short interaction between PH-domain and PtdIns(3,4,5)P_3 contributes to accurate and sensitive gradient-sensing and

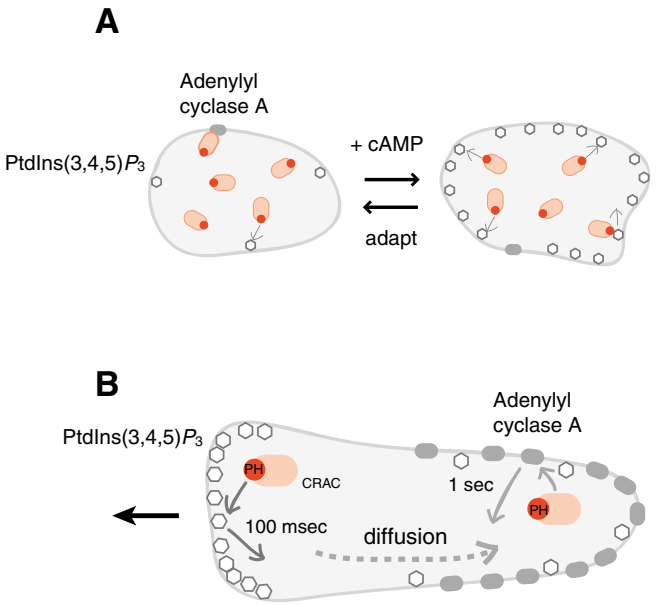

Fig. 7. Overview of the results presented here. (A) Behavior of Crac in cells uniformly stimulated with cAMP. In resting cells, Crac can bind PtdIns(3,4,5)P_3 and ACA-dependent sites. Upon stimulation with cAMP, the amount of PtdIns(3,4,5)P_3 is transiently increased by PI 3-K and PTEN, leading to the transient increments of Crac localisation on membranes and its rapid recycling. (B) Crac undergoing chemotaxis in polarized cells. PtdIns(3,4,5)P_3 and ACA-dependent sites are localized at the pseudopod and the tail of cells, respectively. Since the dissociation of Crac from PtdIns(3,4,5)P_3 is fast, cells can respond rapidly and flexibly to directional changes of gradients. Crac might transmit some signals by freely diffusing into the cytosol from a pseudopod to a tail where ACA is localized.

chemotactic movement. The stable steady-state localization of PH-domain-containing proteins at the leading edge of chemotaxing cells reflects an accumulation of PtdIns(3,4,5)P_3 and the rapid recycling of PH-domain-containing proteins. The fast dissociation from PtdIns(3,4,5)P_3 also suggests that signal transduction processes by PH-domain-containing proteins for pseudopod formation are achieved within ~100 milliseconds on membranes. This might be a general property of signaling components involved in chemotaxis because it takes only a few seconds to respond to stimulation with cAMP by extending a new pseudopod (Swanson and Taylor, 1982).

Recently, it has been reported that PH_{Crac}-GFP can form multiple and distinct accumulations, or patches, on the membrane following the transient recruitment of PH_{Crac}-GFP to the membrane upon uniform stimulation with cAMP (Postma et al., 2004b; Chen et al., 2003). Since these patches were observed with PH_{Crac}-GFP, they would contain only fast dissociation sites, suggesting dynamically maintained structures with a rapid exchange of PH-domain-containing proteins. To demonstrate this, we tried to observe the corresponding increments of Crac-GFP on membranes after stimulation with cAMP in our experimental system. In fact, patches could be observed under EPI-FM. However, we rarely observed the corresponding patches on the basal surface of cells by TIR-FM. Since the visible area under TIR-FM is limited to basal membranes of cells near the surface of the coverslip, the patch formation might not be organized on the basal membrane.

By analyzing Crac-GFP expressed in *aca*-null cells, the slow-dissociation site was identified as ACA itself or a complex depending on the presence of ACA. This suggests a possible interaction between Crac and ACA in living cells. The half-time of the slow-dissociation site was estimated to be ~1 second. However, this value might be too low because photobleaching of the Crac-GFP absorbed on glass surface occurs at the rate of ~4 seconds.

Interesting questions have been raised concerning the function of Crac in ACA activation (Parent et al., 1998; Kriebel et al., 2003). First, the temporal relationship between Crac translocation and ACA activation has apparent contradictions. As shown previously, the majority of Crac molecules are recruited transiently to membranes 5-10 seconds after stimulation with cAMP, whereas ACA starts to be activated ~1 minute after stimulation with cAMP (Parent et al., 1998; Schaffer, 1975; Klein and Darmon, 1977). Second, the spatial relationship between Crac and ACA cannot easily explain the involvement of Crac in ACA activation. Crac and ACA are localized at the leading edge and at the rear end, respectively, of polarized cells undergoing chemotaxis (Parent et al., 1998; Kriebel et al., 2003). However, biochemical and genetic analyses revealed the requirement of Crac on receptor-mediated activation of ACA (Insall et al., 1994; Lilly and Devreotes, 1994; Lilly and Devreotes, 1995; Wang et al., 1999). Crac-null mutants do not show activation of adenylyl cyclase A (ACA) in response to cAMP, but although lysates of Crac-null cells have no activity to regulate adenylyl cyclase A, it can be reconstituted by adding purified Crac to the lysates (Lilly and Devreotes, 1994; Lilly and Devreotes, 1995). By using single-molecule imaging techniques, we found a minor fraction of Crac-GFP in living cells, which were localized preferentially at the rear end of polarized cells and were detected in the late phase after transient recruitments of Crac-GFP upon uniform stimulation with cAMP (Figs 4, 5, 6). These findings suggest that the minor fraction of Crac serves as a regulator of ACA activation.

A slow-dissociation site was observed in unstimulated cells as well as in adapted cells after stimulation with cAMP. However, this does not mean that the slow-dissociation site disappeared from the membrane after stimulation with cAMP, because we cannot exclude the possibility that the slow-dissociation site becomes an insignificant fraction of the total sites owing to the vigorous increase of fast-dissociation sites. In the case of the cell shown in Fig. 3B, on average 1.1 Crac-GFP molecules are bound to the membrane, 0.96 to the fast-dissociation site and 0.14 to the slow-dissociation site. Upon addition of cAMP, the average number of the bound molecules increased to 14.6 in the same cell (6-12 seconds after the stimulation in Fig. 3B). Thus, the number of molecules on the fast-dissociation site increased 15-fold upon stimulation. Assuming that number of molecules on the slow-dissociation site stays the same before and after stimulation, it would be ~1% (0.14/14.6) of the total bound molecules after the stimulation. Indeed, as shown in Fig. 4, there are no detectable differences in the number of molecules on the slow-dissociation site before stimulation with cAMP and after adaptation were detected, suggesting that Crac molecules are already bound to ACA in

unstimulated cells. However, as mentioned above, ACA is not activated in unstimulated cells. Then, what is the signal leading to ACA activation? One speculation is that some undefined factors might be required for Crac-mediated activation of ACA that would not affect on the binding properties of Crac to ACA.

Two different binding sites for Crac might be important in regulating ACA activation temporally and spatially. As outlined above, assuming that PtdIns(3,4,5)P_3-Crac complexes move from pseudopod to tail (~20 μm) by lateral diffusion, it would take ~17 minutes. On the other hand, Crac dissociated from a pseudopod can reach to the tail within 10 seconds by freely diffusing in the cytosol (Ruchira et al., 2004). Thus, by dissociating from membrane, Crac can move rapidly from the leading edge to the rear end where ACA is located. This might be important for the aggregation processes of *D. discoideum* cells during development. The aggregation is achieved by an elaborate combination of two events: chemotaxis and cAMP relay (Weijer, 2004). *D. discoideum* cells move towards the higher concentration of cAMP by chemotaxis and then produce cAMP by ACA activation for cAMP relay. Because the temporal order of the two events is crucial for cells to form aggregates, chemotactic signaling events and cAMP relay should be matched temporally in cells, suggesting some mechanisms underlying the temporal order. One possible mechanism is to transmit some signals from the chemotactic signaling system to the relay system of cAMP. Transient binding of Crac to the pseudopod membrane, and its dissociation into cytosol might be important to interact with other components for ACA activation such as Pianissimo (Chen et al., 1997). It is worth examining by single-molecule imaging techniques the membrane association of other components involved in ACA activation.

Materials and Methods

Cell culture and development

Ax2 cells and the mutant cell lines described below were grown at 21°C in HL5 medium supplemented with 5 ng/ml vitamin B12 and 100 ng/ml folic acid (Watts and Ashworth, 1970). The transformants expressing Crac fused to GFP (Crac-GFP) or the PH-domain of Crac fused to GFP (PH_{Crac}-GFP) were selected with 20 μg of G418/ml. Ax2 cells with a disrupted adenylyl cyclase A gene (*aca*) (see below) were selected and maintained in the presence of blasticidin S at 10 μg/ml. Cells were starved for up to 6 hours in a plastic dish after having been washed and resuspended in development buffer (DB; 5 mM Na_2HPO_4, 5 mM NaH_2PO_4, 2 mM $MgSO_4$, 0.2 mM $CaCl_2$, pH 6.0) at a density of 2×10^6 cells/ml. Mutant a*c*a-null cells were starved in DB for 1 hour and then incubated for another 5 hours in the presence of pulses of 10 mM cAMP given every 6 minutes (Devreotes et al., 1987).

Gene disruption and transformation

Ax2 cells with a disrupted *aca* gene was obtained by homologous recombination. The construct was generated by fusion PCR using four primers; primer 1 (5′-GTCTTCAATATTCAATAAGTTG-3′), primer 2 (5′-GTAATCATGGTCATA-GCTGTTTCCTGCAGGTGGTAGATAATTGAAGCGTAC-3′), primer 3 (5′-CACTGGCCGTCGTTTTACAACGTCGACCATATTCTTAGAATCAACACTCG-3′) and primer 4 (5′-CATCTAAATTGTACTTGAATACC-3′). Two DNA fragments were amplified using genomic DNA as template. One of them, 5′-ACA, corresponds to the region upstream of the *aca* open reading frame, which was amplified with primers 1 and 2. The other, 3′-ACA, corresponds to the region encoding the middle part of *aca* and was amplified with primers 3 and 4. The blasticidin resistance (bsr) cassette was also amplified with primers 2 and 3. According to the method of Kuwayama, fusion PCR was performed using the three amplified fragments and primers 1 and 4 (Kuwayama et al., 2002). Thus, we obtained the disruption construct in which 5'-ACA, the bsr cassette and 3'-ACA were, in this order, connected. The construct was introduced by electroporation into exponentially growing Ax2 cells, according to the method of Howard et al. (Howard et al., 1988). The gene disruption was confirmed by PCR using genomic DNA as template.

Single-molecule imaging in living *D. discoideum* cells

Starved cells were washed and suspended in DB, and an aliquot was placed on a glass cover slip. After they had settled, cells were overlaid with a sheet of agarose (Fukui et al., 1987). In certain experiments that required an increment in the concentration of cAMP, caged cAMP (Dojindo, Kumamoto, Japan) was contained in the agarose sheet at 1 mM. For fixation, the glass coverslip was soaked for 15 minutes with DB supplemented with 3.7% formaldehyde and then washed in DB. Single molecules of Crac-GFP or PH_{Crac}-GFP were visualized using an objective-type total internal reflection microscope constructed on an inverted fluorescence microscope (IX70, Olympus, Japan) (Ueda et al., 2001). Specimens were illuminated with a Kr-Ar laser (488 nm) (643-RYB, Melles Griot, Japan) through an objective lens (PlanApo 60×, NA 1.45, Olympus). The configuration is illustrated in Fig. 2. The laser beam was passed through a beam expander (BE, LBED, Sigma Koki, Japan), neutral density filter (ND, Sigma Koki), quarter-wave plate (λ/4, WPQ 5900-4M, Sigma Koki) and a band pass filter (BP470-490, Olympus), and was focused on the back focal plane of the objective lens with a focusing lens (L) and a mirror (M). By adjusting the angle and position of the mirror, the settings can be switched between epifluorescence microscopy (EPI-FM) and total internal reflection fluorescence microscopy (TIR-FM) (Tokunaga et al., 1997). Fluorescence signals from Crac-GFP were collected with the objective lens and selected with a dichroic mirror (DM2, DM500, Olympus) and emission filter (EF, BA510-550, Olympus) and focused by focusing optics of IX-70 (FO) on the camera. The images were intensified with image intensifier (II, GaAsP, C8600-05, Hamamatsu Photonics, Japan) and acquired with an EB-CCD camera (C7190-23, Hamamatsu Photonics). For photolysis of caged cAMP, ultraviolet light was introduced into the objective lens from a high-voltage mercury lamp through a dichroic mirror. UV light was irradiated uniformly at a small region near the cell of interest. The spatial limitation in the depth of the observation depends on the penetration depth of evanescent field generated by total internal reflerection (Axelrod, 2001; Wazawa and Ueda, 2005). The penetration depth where the intensity of evanescent field becomes 1/*e* can be estimated from wavelength, refractive index of coverslip and specimen, and incident angle of excitation laser. In our apparatus, it should be ~100 nm from the surface of the coverslips, and thus only the basal membrane of the cells was illuminated by the excitation light.

Data analysis of single molecules

Images of single Crac-GFP molecules were taken at a rate of 33-milliseconds/frame and stored as a stack of frames on a personal computer. Individual fluorescent spots were followed semi-automatically, and the positions (*x* and *y* coordinates), the fluorescence intensities and the frames were determined. The lifetime of individual Crac-GFP molecules was obtained by measuring the duration between the appearance and the disappearance of the fluorescent spots on membrane. The dissociation rates of Crac were obtained by fitting the distribution of the lifetimes to a sum of exponential decay curves, $a_1\exp[-k_1t]+a_2\exp[-k_2t]$, where k_i and a_i are dissociation rates and the relative amounts of the i^{th} components [Sakmann and Neher, 1995; Ueda et al., 2001]. τ, the average lifetime of Crac molecules, is the reversed value of k.

This study was supported by MEXT's Leading Project.

References

Axelrod, D. (2001). Total internal reflection fluorescence microscopy in cell biology. *Traffic* **2**, 764-774.

Bourne, H. R. and Weiner, O. (2002). A chemical compass. *Nature* **419**, 21.

Chen, L., Janetopoulos, C., Huang, Y. E., Iijima, M., Borleis, J. and Devreotes, P. N. (2003). Two phases of Actin polymerization display different dependencies on PI(3,4,5)P_3 accumulation and have unique roles during chemotaxis. *Mol. Biol. Cell* **14**, 5028-5037.

Chen, M. Y., Long, Y. and Devreotes, P. N. (1997). A novel cytosolic regulator, Pianissimo, is required for chemoattractant receptor and G protein-mediated activation of the 12 transmembrane domain adenylyl cyclase in Dictyostelium. *Genes Dev*. **11**, 3218-3231.

Comer, F. I. and Parent, C. A. (2002). PI 3-kinases and PTEN: how opposites chemoattract. *Cell* **109**, 541-544.

Comer, F. I., Lippincott, C. K., Masbad, J. J. and Parent, C. A. (2005). The PI3K-mediated activation of CRAC independently regulates Adenylyl cyclase activation and chemotaxis. *Curr. Biol*. **15**, 134-139.

Devreotes, P. N. and Zigmond, S. H. (1988). Chemotaxis in eukaryotic cells: a focus on leukocytes and Dictyostelium. *Annu. Rev. Cell Biol.* **4**, 649-686.

Devreotes, P., Fontana, D., Klein, P., Sherring, J. and Theibert, A. (1987). Transmembrane signaling in Dictyostelium. *Methods Cell Biol*. **28**, 299-331.

Dickson, R. M., Cubitt, A. B., Tsien, R. Y. and Moerner, W. E. (1997). On/off blinking and switching behaviour of single molecules of green fluorescent protein. *Nature* **388**, 355-358.

Dormann, D., Weijer, G., Dowler, S. and Weijer, C. J. (2004). In vivo analysis of 3-phosphoinositide dynamics during Dictyostelium phagocytosis and chemotaxis. *J. Cell Sci.* **117**, 6497-6509.

Fisher, P. R., Merkl, R. and Gerisch, G. (1989). Quantitative analysis of cell motility and chemotaxis in Dictyostelium discoideum by using an image processing system and

a novel chemotaxis chamber providing stationary chemical gradients. *J. Cell Biol*. **108**, 973-984.

Fukui, Y., Yumura, S. and Yumura, T. K. (1987). Agar-overlay immunofluorescence: high-resolution studies of cytoskeletal components and their changes during chemotaxis. *Methods Cell Biol.* **28**, 347-356.

Funamoto, S., Meili, R., Lee, S., Parry, L. and Firtel, R. A. (2002). Spatial and temporal regulation of 3-phosphoinositides by PI 3-kinase and PTEN mediates chemotaxis. *Cell* **109**, 611-623.

Funatsu, T., Harada, Y., Tokunaga, M., Saito, K. and Yanagida, T. (1995). Imaging of single fluorescent molecules and individual ATP turnovers by single myosin molecules in aqueous solution. *Nature* **374**, 555-559.

Haugh, J. M., Codazzi, F., Teruel, M. and Meyer, T. (2000). Spatial sensing in fibroblasts mediated by 3′ phosphoinositides. *J. Cell Biol*. **151**, 1269-1280.

Hibino, K., Watanabe, T. M., Kozuka, J., Iwane, A. H., Okada, T., Kataoka, T., Yanagida, T. and Sako, Y. (2003). Single- and multiple-molecule dynamics of the signaling from H-Ras to cRaf-1 visualized on the plasma membrane of living cells. *Chemphyschem* **4**, 748-753.

Howard, P. K., Ahern, K. G. and Firtel, R. A. (1988). Establishment of a transient expression system for Dictyostelium discoideum. *Nucleic Acids Res*. **16**, 2613-2623.

Huang, Y. E., Iijima, M., Parent, C. A., Funamoto, S., Firtel, R. A. and Devreotes, P. N. (2003). Receptor-mediated regulation of PI3Ks confines PI(3,4,5)P3 to the leading edge of chemotaxing cells. *Mol. Biol. Cell* **14**, 1913-1922.

Iijima, M. and Devreotes, P. N. (2002). Tumor suppressor PTEN mediates sensing of chemoattractant gradients. *Cell* **109**, 599-610.

Iijima, M., Huang, Y. E. and Devreotes, P. N. (2002). Temporal and spatial regulation of chemotaxis. *Dev. Cell* **3**, 469-478.

Iino, R., Koyama, I. and Kusumi, A. (2001). Single molecule imaging of green fluorescent proteins in living cells: E-cadherin forms oligomers on the free cell surface. *Biophys. J.* **80**, 2667-2677.

Insall, R., Kuspa, A., Lilly, P. J., Shaulsky, G., Levin, L. R., Loomis, W. F. and Devreotes, P. (1994). CRAC, a cytosolic protein containing a Pleckstrin homology domain, is required for receptor and G protein-mediated activation of Adenylyl cyclase in Dictyostelium. *J. Cell Biol*. **126**, 1537-1545.

Ishijima, A. and Yanagida, T. (2001). Single molecule nanobioscience. *Trends Biochem. Sci*. **26**, 438-444.

Jacobson, K., Ishihara, A. and Inman, R. (1987). Lateral diffusion of proteins in membranes. *Annu. Rev. Physiol*. **49**, 163-175.

Janetopoulos, C., Jin, T. and Devreotes, P. (2001). Receptor-mediated activation of heterotrimeric G-proteins in living cells. *Science* **291**, 2408-2411.

Janetopoulos, C., Ma, L., Devreotes, P. N. and Iglesias, P. A. (2004). Chemoattractant-induced phosphatidylinositol 3,4,5-trisphosphate accumulation is spatially amplified and adapts, independent of the actin cytoskeleton. *Proc. Natl. Acad. Sci. USA* **101**, 8951-8956.

Jin, T., Zhang, N., Long, Y., Parent, C. A. and Devreotes, P. N. (2000). Localization of the G protein betagamma complex in living cells during chemotaxis. *Science* **287**, 1034-1036.

Kimmel, A. R. and Parent, C. A. (2003). The signal to move: *D. discoideum* go orienteering. *Science* **300**, 1525-1527.

Klein, C. and Darmon, M. (1977). Effects of cyclic AMP pulses on adenylyl cyclase and the phosphodiesterase inhibitor of Dictyostelium discoideum. *Nature* **268**, 76-78.

Kriebel, P. W., Barr, V. A. and Parent, C. A. (2003). Adenylyl cyclase localization regulates streaming during chemotaxis. *Cell* **112**, 549-560.

Kuwayama H, Obara S, Morio T, Katoh M, Urushihara H and Tanaka Y. (2002). PCR-mediated generation of a gene disruption construct without the use of DNA ligase and plasmid vectors. *Nucleic Acids Res.* **30**, E2.

Lilly, P. J. and Devreotes, P. N. (1994). Identification of CRAC, a cytosolic regulator required for guanine nucleotide stimulation of Adenylyl cyclase in Dictyostelium. *J. Biol. Chem*. **269**, 14123-14129.

Lilly, P. J. and Devreotes, P. N. (1995). Chemoattractant and GTPγS-mediated stimulation of Adenylyl cyclase in Dictyostelium requires translocation of CRAC to membranes. *J. Cell Biol.* **129**, 1659-1665.

Mato, J. M., Losada, A., Nanjundiah, V. and Konijn., T. M. (1975). Signal input for a chemotactic response in the cellular slime mold Dictyostelium discoideum. *Proc. Natl. Acad. Sci. USA* **72**, 4991-4993.

Meili, R., Ellsworth, C., Lee, S., Reddy, T. B., Ma, H. and Firtel, R. A. (1999). Chemoattractant-mediated transient activation and membrane localization of Akt/PKB is required for efficient chemotaxis to cAMP in Dictyostelium. *EMBO J.* **18**, 2092-2105.

Parent, C. A. (2004). Making all the right moves: chemotaxis in neutrophils and Dictyostelium. *Curr. Opin. Cell Biol*. **16**, 4-13.

Parent, C. A. and Devreotes, P. N. (1999). A cell's sense of direction. *Science* **284**, 765-770.

Parent, C. A., Blacklock, B. J., Froehlich, W. M., Murphy, D. B. and Devreotes, P. N. (1998). G protein signaling events are activated at the leading edge of chemotactic cells. *Cell* **95**, 81-91.

Postma, M., Bosgraaf, L., Loovers, H. M. and van Haastert, P. J. (2004a). Chemotaxis: signalling modules join hands at front and tail. *EMBO Rep*. **5**, 35-40.

Postma, M., Roelofs, J., Goedhart, J., Loovers, H. M., Visser, A. J. and Van Haastert, P. J. (2004b). Sensitization of Dictyostelium chemotaxis by phosphoinositide-3-kinase-mediated self-organizing signalling patches. *J. Cell Sci.* **117**, 2925-2935.

Ridley, A. J., Schwartz, M. A., Burridge, K., Firtel, R. A., Ginsberg, M. H., Borisy, G., Parsons, J. T. and Horwitz, A. R. (2003). Cell migration: integrating signals from front to back. *Science* **302**, 1704-1709.

Ruchira, Hink, M. A., Bosgraaf, L., van Haastert, P. J. and Visser, A. J. (2004). Pleckstrin homology domain diffusion in Dictyostelium cytoplasm studied using fluorescence correlation spectroscopy. *J. Biol. Chem*. **279**, 10013-10019.

Sakmann, B. and Neher, E. (1995). *Single Channel Recording*. New York: Plenum Press.

Sako, Y., Minoguchi, S. and Yanagida, T. (2000a). Single-molecule imaging of EGFR signaling on the surface of living cells. *Nat. Cell Biol*. **2**, 168-172.

Sako, Y., Hibino, K., Miyauchi, T., Miyamoto, Y., Ueda, M. and Yanagida, T. (2000b). Single-molecule imaging of signaling molecules in living cells. *Single Mol*. **1**, 159-163.

Sako, Y. and Yanagida, T. (2003). Single-molecule visualization in cell biology. *Nat. Rev. Mol. Cell. Biol*. Suppl. SS1-SS5.

Saxton, M. J. and Jacobson, K. (1997). Single-particle tracking: applications to membrane dynamics. *Annu. Rev. Biophys. Biomol. Struct*. **26**, 373-399.

Schaffer, B. M. (1975). Secretion of cAMP induced cAMP in the cellular slime mold Dictyostelium discoideum. *Nature* **255**, 549-552.

Servant, G., Weiner, O. D., Herzmark, P., Balla, T., Sedat, J. W. and Bourne, H. R. (2000). Polarization of chemoattractant receptor signaling during neutrophil chemotaxis. *Science* **287**, 1037-1040.

Swanson, J. A. and Taylor, D. L. (1982). Local and spatially coordinated movements in Dictyostelium discoideum amoebae during chemotaxis. *Cell* **28**, 225-232.

Tokunaga, M., Kitamura, K., Saito, K., Iwane, A. H. and Yanagida, T. (1997). Single-molecule imaging of fluorophores and enzymatic reactions achieved by objective-type total internal reflection fluorescence microscopy. *Biochem. Biophys. Res. Comm*. **235**, 47-53.

Ueda, M., Sako, Y., Tanaka, T., Devreotes, P. N. and Yanagida, T. (2001). Single-molecule analysis of chemotactic signaling in Dictyostelium cells. *Science* **294**, 864-867.

Wang, B., Shaulsky, G. and Kuspa, A. (1999). Multiple developmental roles for Crac, a cytosolic regulator of adenylyl cyclase. *Dev. Biol*. **208**, 1-13.

Watanabe, N. and Mitchison, T. J. (2001). Single-molecule speckle analysis of actin filament turnover in lamellipodia. *Science* **295**, 1083-1086.

Watts, D. J. and Ashworth, J. M. (1970). Growth of myxamoebae of the cellular slime mould Dictyostelium discoideum in axenic culture. *Biochem. J.* **119**, 171-174.

Wazawa, T. and Ueda, M. (2005). Total internal reflection fluorescence microscopy in single molecule nanobioscience. *Adv. Biochem. Eng. Biotechnol.* **95**, 77-106.

Weijer, C. J. (2004). Dictyostelium morphogenesis. *Curr. Opin. Genet. Dev*. **14**, 392-398.

Xiao, Z., Zhang, N., Murphy, D. B. and Devreotes, P. N. (1997). Dynamic distribution of chemoattractant receptors in living cells during chemotaxis and persistent stimulation. *J. Cell Biol*. **139**, 365-374.

Journal of Cell Science